

## IMPLEMENTATION OF SIMPLIFIED CHEMICAL KINETICS BASED ON INTRINSIC LOW-DIMENSIONAL MANIFOLDS

U. MAAS

*Institut für Technische Verbrennung, Universität Stuttgart  
Pfaffenwaldring 12, W-7000 Stuttgart 80, Germany*

AND

S. B. POPE

*Sibley School of Mechanical and Aerospace Engineering  
Cornell University, Ithaca, N.Y. 14853-7501 USA*

A general procedure for simplifying chemical kinetics and its use in reacting flow models is developed, which is based on the dynamical systems approach. In contrast to conventional reduced mechanisms no information is required concerning which reactions are to be assumed to be in partial equilibrium nor which species are assumed to be in steady state. Based on a local eigenvector analysis, the method identifies the fast time scales of the chemical reaction systems, which differ typically by orders of magnitude. Assuming that the fastest relaxation processes in chemical reactions proceed infinitely fast (i.e., are in local equilibrium), it is then possible to reduce the state space globally, such that it can be described by means of only a small number of reaction progress variables. The only "inputs" to the procedure are the detailed kinetics mechanism and the number of degrees of freedom required in the simplified scheme. Then the state properties given by the simplified scheme are automatically determined as functions of the coordinates associated with the degrees of freedom. A tabulation procedure allows an efficient use of the results in CFD codes. Furthermore a general procedure for coupling the reduced mechanism with other than chemical processes like flow and molecular transport is discussed. Results are presented for the CO/H<sub>2</sub>/air system both for a simple homogeneous closed system and a flow reactor.

### Introduction

There are now many examples (e.g., Ref. 1–4) of successful computations of simple laminar flames using detailed chemical kinetics schemes. Such schemes typically involve 40 species which participate in several hundred reactions. In most practical combustion problems there are additional complicating factors such as geometric complexity and turbulence. For many decades to come, computing power will remain inadequate to handle these complexities in conjunction with detailed kinetics. Consequently there has been considerable interest in the development of simplified kinetic schemes (see e.g. Ref. 5 for references) that have much lower computational requirements.

Recently we<sup>6,7</sup> developed a new methodology—the Intrinsic Low-Dimensional Manifold (ILDM) method—for generating simplified kinetic schemes, based on ideas from dynamical systems. This approach, though different (see Ref. 6, 7), uses similar methods as the computational singular perturbation method developed by Lam et al.<sup>8,9</sup> The two

contributions of this paper are: to describe an efficient computational implementation of the scheme; and, by comparison with detailed kinetics calculations, to demonstrate the accuracy of the scheme as a whole for a perfectly-stirred reactor test (which includes extinction).

In general, in a simplified kinetics scheme, the thermochemical state of the fluid is represented by a small number ( $N$ ) of variables—typically less than five—which we denote by  $\theta = \{\theta_1, \theta_2, \dots, \theta_N\}$ . These variables may correspond to species mass fractions, though they need not. Then, by assumption, the density  $\rho(\theta)$ , the temperature  $T(\theta)$ , and the mass fraction of the general species  $\alpha$ ,  $w_\alpha(\theta)$  are known functions of  $\theta$ .

In a fluid flow, the composition field  $\theta(\mathbf{x}, t)$  evolves by

$$\frac{\partial}{\partial t} \theta(\mathbf{x}, t) = \mathcal{S}(\theta[\mathbf{x}, t]) + \mathcal{I}(\mathbf{x}, t). \quad (1)$$

Here  $\mathcal{S}(\theta)$  is the rate of change of  $\theta$  due to chemical reaction, while  $\mathcal{I}(\mathbf{x}, t)$  denotes the rate of change

due to all other effects—convection, molecular diffusion etc. The simplified scheme determines  $\underline{S}(\theta)$ .

In the numerical solution of the governing equations for a combustion problem (e.g. Eq. (1)), functions such as  $\rho(\theta)$  and  $\underline{S}(\theta)$  have to be evaluated many times—perhaps  $10^7$  times in a pdf/Monte-Carlo calculation—and consequently it is essential that this can be done economically. The method used<sup>10,11</sup> is, first, to tabulate the required functions, and then to perform the evaluations by interpolation in the table.

There is no inherent reason why, in the long run, the whole procedure cannot be automated—the generation of the reduced scheme, the table set-up, and the interpolation. While not fully automated at present, the Intrinsic Low-Dimensional Manifold (ILDM) method generates a near-optimal reduced scheme, with an absolute minimum of input: this is briefly reviewed in the next section. In the third section an automatic tabulation and interpolation method is described. This uses adaptive gridding to generate unstructured tables that ensure that subsequent interpolation errors are less than a specified tolerance. In the fourth section the method is applied to a PSR (perfectly stirred reactor) test problem. The results demonstrate both the accuracy of the simplified scheme, and also the computational economy of the tabulation procedure.

### Mathematical Model

The mathematical model for gas-phase chemical reaction systems consists of a set of partial differential equations, namely the conservation equations, which describes the time-dependent development of all the properties that determine the state of the system (e.g., species mass fractions, specific enthalpy, pressure and velocity field). The governing processes (i.e., flow, molecular transport and chemical reaction) occur at time-scales which differ by orders of magnitude. In combustion processes chemical reaction is usually governed by time-scales ranging from  $10^{-9}$  to  $10^{+2}$  s. If we look at a typical spectrum of time-scales as it occurs in flames, it can be seen that the chemical time scales cover a larger range than the so-called physical time scales (representing, e.g., molecular transport). The very fast time scales in chemical kinetics usually are responsible for equilibration processes (reactions are in partial equilibrium, species are in steady state). If we make use of the fact that those time scales are very fast, it is possible to decouple them. In this section we briefly outline the method we use to decouple slow from fast chemical time scales for the case of a homogeneous, adiabatic, isobaric closed system (details can be found in<sup>6,7</sup>). The coupling of

the method with physical processes like diffusion will be discussed in the fourth section.

The state of a spatially homogeneous, adiabatic, isobaric closed system is completely determined by  $n_s + 2$  variables (where  $n_s$  denotes the number of species in the reaction system), namely by the enthalpy, the pressure and the mass fractions. Thus the state of the chemical system is given as a point in an  $n(= n_s + 2)$ -dimensional state space. The governing equation system reads:

$$\begin{aligned} \frac{\partial h}{\partial t} &= 0 & \frac{\partial P}{\partial t} &= 0 \\ \frac{\partial \phi_i}{\partial t} &= \Omega_i & \Omega_i &= \frac{\omega_i(h, P, \underline{\phi})}{\rho(h, P, \underline{\phi})} \end{aligned} \quad (2)$$

or in vector formulation:

$$\frac{\partial}{\partial t} \underline{\psi} = \underline{F}(\underline{\psi}) \quad (3)$$

with  $\underline{\psi} = (h, P, \phi_1, \phi_2, \dots, \phi_{n_s})^T$  and  $\underline{F}(\underline{\psi}) = (0, 0, \Omega_1, \Omega_2, \dots, \Omega_{n_s})^T$ . In these equations  $\phi_i$  denotes the specific mole number of species  $i$ , which is defined by:  $\phi_i = w_i/M_i$ ,  $w_i$ , the mass fraction of species  $i$ ,  $M_i$  the molar mass of species  $i$ ,  $h$  the specific enthalpy,  $P$  the pressure and  $\omega_i$  the molar rate of production of species  $i$ . Furthermore, if we make use of the fact that the system is closed, adiabatic and isobaric, it follows that chemical reaction takes place in a linear subspace of dimension  $n_r(= n_s - n_e)$ , the so-called reaction space, corresponding to fixed values of enthalpy, pressure and element composition ( $n_e$  = number of elements). Chemical reaction corresponds to a movement along trajectories in the reaction space, governed by the chemical rate equations. Because of the large differences in the chemical time scales, usually the behaviour of a reaction system can be separated into two different processes: Processes which occur at slow or intermediate time scales and very fast equilibration processes (which in chemical terms correspond, e.g., to reactions in partial equilibrium or species in steady state).

This behaviour can be nicely seen in a plot of trajectories (obtained by detailed chemistry calculations) in the state space of a chemical reaction system. Shown in Fig. 1 is a projection into the  $\text{CO}_2/\text{H}$ -plane for a  $\text{CO}/\text{H}_2/\text{air}$  combustion system at fixed values of enthalpy, pressure and element composition. It can be seen that (starting at arbitrary initial conditions), all the different trajectories approach (after some fast relaxation process) some lower-dimensional subspace, in which reaction proceeds only according to slow time scales. That means chemical reaction can be separated into fast processes, attracting the system to a low-dimensional

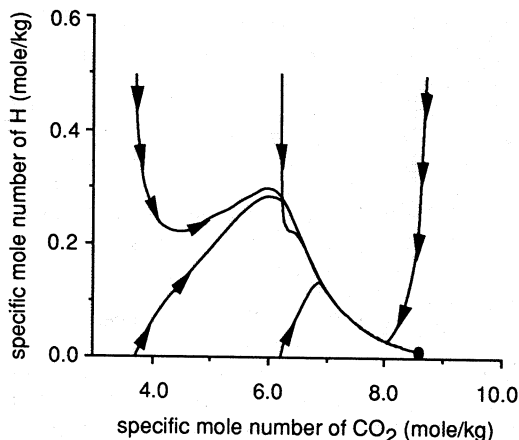


FIG. 1. Sample trajectories in the state space for a CO/H<sub>2</sub>/air system ● denotes the equilibrium value; projection into the CO<sub>2</sub>-H plane.

subspace and slow processes, governing the movement within this subspace. If we are not interested in the details of the relaxation processes (occurring at very short time scales), but only in the slow time scales, we can confine chemistry to those low-dimensional manifolds and describe the whole chemical reaction system by a much smaller number of variables.

The basic task is now to identify these low-dimensional subspaces of the reaction space, where local equilibrium with respect to the fastest time scales exists. This can be done by an analysis of the Jacobian  $J$  of the system ( $J_{ij} = \partial F_i / \partial \psi_j$ ). Analyzing Eq. (3) it can be seen, that locally (i.e. at all points in the state space there exist  $n$  characteristic time scales and associated with those time scales  $n$  characteristic directions (eigenvalues and eigenvectors of the local Jacobian, see<sup>6,7</sup> for details). Starting at some point in the state space, the fast relaxation processes (corresponding to eigenvalues  $\ll 0$ ) will lead the system to points in the state space, where there is local equilibrium with respect to the fastest time scales. Then the system will evolve further. The relaxation processes will always (during the reaction) move the system back to states with local equilibrium. Thus, if we identify the points in state space where local equilibrium with respect to the  $n_f$  fastest relaxing time scales exists, we identify the low-dimensional manifold of dimension  $N = n - n_f$  with the property that movements within this manifold correspond to slow time scales and we can confine chemistry to movements within this manifold. The manifold can be parametrized by  $N$  variables. In simple case those parameters  $\theta_i$  might e.g. be the mass fractions of some species, however, the manifold does not depend on the parametrization.

See Ref. 6, 7 for a detailed mathematical formulation of the method.

### Tabulation of the Chemical Rates of Production

Having developed the method needed to identify the low-dimensional manifolds in composition space, there is need of a numerical method in order to use the results for a simplified treatment of the chemical kinetics. Noting that the low-dimensional manifold can be parametrized by a small number ( $N$ ) of variables  $\theta = (\theta_1, \theta_2, \dots, \theta_N)$ , the governing equation system (3) can be transformed into a parametrized form (cf. eq. (1):

$$\frac{\partial}{\partial t} \theta = \underline{S}(\theta), \quad (4)$$

describing the change of the parameters  $\theta$  with time, i.e. the movement within the manifold. The advantage of this formulation is that the dimension ( $N$ ) of this equation system is usually much smaller than that of the full equation system.

If we tabulate  $\underline{S}(\theta)$  as functions of the parameters  $\theta$ , we can integrate Eq. (4) numerically with the aid of a table lookup. However, there might be ranges of the parameters, where  $\underline{S}(\theta)$  depends crucially on  $\theta$ , whereas for other values of the parameters the rates of change depend only slightly on  $\theta$ . A straight forward approach, namely an equidistributed table would either lead to a low accuracy or (for a very fine mesh) to an unnecessary amount of stored information. Thus, a locally refined table setup should be performed. There are two principle problems which have to be addressed. First the determination of the region in the state space, which has to be tabulated and second the method of the local mesh refinement.

The maximum region which has to be tabulated can be determined if we identify the maximum range of parameter values, for which physically reasonable states (i.e. mass fractions positive and smaller than one; pressure and temperature positive etc. (see<sup>6,7</sup>) exist at all. This can be done by a standard simplex method<sup>12</sup> and shall not be described in detail. The results of this procedure are upper and lower bounds for the parameters  $\theta$ , namely  $\theta_{min}$  and  $\theta_{max}$ , where *min* and *max* denote the vectors composed of the minima and maxima of the components  $\theta_i$  respectively. However, for specific combustion problems, the region of tabulation might also be confined to a smaller parameter range.

The method of local mesh refinement that we use starts with an  $N$ -dimensional coarse grid within the bounds  $\theta_{min}$  and  $\theta_{max}$ . The mesh refinement can be applied generally to multidimensional grids. It is basically independent of the structure of the coarse

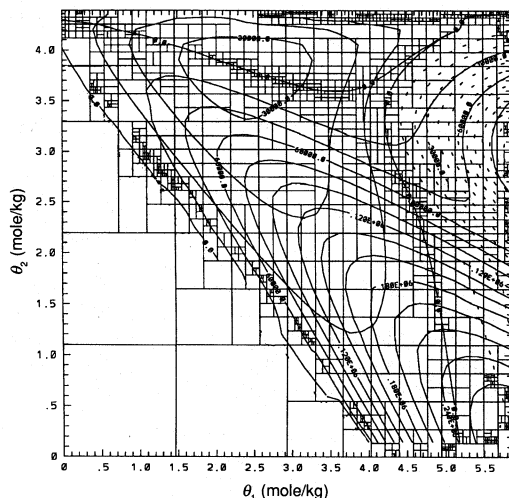


FIG. 2. Locally refined two-dimensional tabulation mesh, contour lines: rates of change of the parameters, ( $d\theta_1/dt = d\phi_{\text{CO}_2}/dt$ ,  $d\theta_2/dt = d\phi_{\text{H}_2\text{O}}/dt$ ); see text for details.

grid. Thus, let us just consider one cell of the coarse grid in the following. The basic criterion for the grid refinement is given by the accuracy of the interpolation within one cell. Let  $\theta_i$  be the tabulation coordinates and  $p(\theta)$  be some associated properties (e.g., the state variables, the rate of change of the parameters etc.). Let furthermore  $\tilde{p}(\theta)$  be the values of the properties obtained by multi-linear cell interpolation. If we look at one cell of the coarse grid, the algorithm for the refinement procedure can be outlined as follows: First the values of  $p$  and  $\tilde{p}$  are evaluated at the cell centre. If the weighted norm  $\|p - \tilde{p}\|_\infty$  is smaller than a specified tolerance  $\epsilon$ , no refinement of the cell is performed. Otherwise the best direction for a cell refinement is determined. The use of a weighted norm allows to control the refinement. Weighting, e.g., the error by the absolute values of the properties, allows to obtain a high accuracy even in regions, where the properties are small in magnitude (see Fig. 2). In one refinement step a cell is allowed to be divided in one dimension of the table into two equally sized children cells. Having generated two children cells out of one parent cell, the procedure is repeated for the children cells until either the required accuracy is obtained or some minimum mesh size has been reached. The result of this procedure is a binary tree of parent and children cells. In the table lookup, this corresponds to a binary search tree. Having determined the coarse cell in which the point of interest is located, the tree can be followed down to the finest grid level, i.e. the fine cell containing

the point can be identified. Within this cell, the values of the properties ( $p(\theta)$ ) can be approximated by multi-linear interpolation.

Fig. 2 shows a two-dimensional table generated by this procedure. The system considered here is a CO/H<sub>2</sub> air system corresponding to a 6/10 mixture of syngas (40 Vol. % CO, 30 Vol. % H<sub>2</sub>, 30 Vol. % N<sub>2</sub>) and air at 300 K and 1 bar. Input to the manifold and table setup procedure has been a detailed reaction mechanism consisting of 13 species and 67 elementary reactions.<sup>13</sup>

As parameters, the specific mole numbers of CO<sub>2</sub> and H<sub>2</sub>O have been chosen for convenience (i.e.,  $\theta_1 = \phi_{\text{CO}_2}$ ,  $\theta_2 = \phi_{\text{H}_2\text{O}}$ ), the element composition, enthalpy and pressure are fixed and thus do not form additional dimensions of the table. (It shall be noted once more that the manifolds themselves are independent of the choice of the parameters). The table has been generated allowing a tolerance  $\epsilon = 1\%$ , a maximum refinement depth of 6 (referring to the maximum number of refinement levels of one coarse cell). The fine grid consists of 4604 cells and 2989 vertices. For the sample calculations presented below, an even finer grid ( $\epsilon = 0.5\%$ ) has been chosen in order to minimize interpolation errors such that the results presented below do not depend on the accuracy of the table. In fact much coarser grids can be used without much loss of accuracy.<sup>14</sup> The criterion for the grid refinement is the accuracy of the magnitude of the rate of change of the parameters in this case, which is included in the diagram as contour lines. It can be seen that the mesh is refined in regions, where the reaction progress rates change nonlinearly. In the table, for given values of  $\theta$ , the rate of change of the parameters are stored as well as the values of the state space and some other information (see below) and can be used for an efficient integration of the rate equations.

Figure 3 finally shows a comparison of results obtained using detailed chemical kinetics (15-dimensional state space) to integrate the rate equations and the two-dimensional intrinsic manifold described above. The starting value is a point on the manifold corresponding to  $\theta_1 = \phi_{\text{CO}_2} = 3$  and  $\theta_2 = \phi_{\text{H}_2\text{O}} = 2$  which corresponds to an initial temperature of about 1240 K. Both, reduced and detailed chemical rate equations were integrated using an implicit extrapolation code.<sup>15</sup> Plotted are the specific mole numbers of CO<sub>2</sub>, H<sub>2</sub>O, OH and O versus the time. In fact the method does not only reproduce the major species (CO<sub>2</sub> and H<sub>2</sub>O), but a similarly good agreement is obtained for reactive species like OH and O radicals. The small discrepancies in the early stage of the reaction can be explained by the fact, that during that period the gap between slow and fast time scales is quite narrow, leading to a coupling of those time scales, which

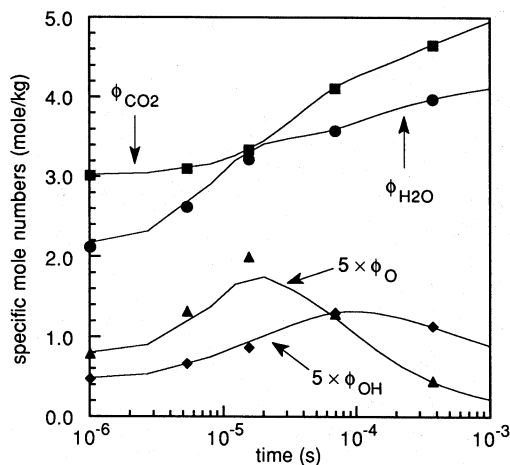


FIG. 3. Plot of the specific mole numbers of  $\text{CO}_2$ ,  $\text{H}_2\text{O}$ ,  $\text{O}$  and  $\text{OH}$  versus time for a  $\text{CO}/\text{H}_2/\text{air}$  system (see text for details on the reaction system and the initial values); lines denote detailed chemical kinetics, symbols denote the reduced kinetics results.

are, at the same time, of the order of the overall time scale of the chemical reaction.

### Coupling of Chemistry with Physical Processes

In the last chapter it has been shown that the method of constructing intrinsic low-dimensional manifolds in composition space can be used to simplify chemical kinetics and thus, the solution of the chemical rate equations. However, most interesting reacting flow problems involve the coupling of chemical kinetics with other processes like flow and molecular transport. Now, all those physical processes can be viewed as disturbances of the chemical reaction system (which may, indeed be very large). In the context of the geometrical representation of chemical kinetics all those processes do the same thing: they move the state either within the low-dimensional manifolds or off the manifold. The consequences for the chemical reaction system can be explained by means of a simple diagram (Fig. 4). Let us assume that we are at a point  $\psi_0$  on the manifold and that there is some perturbation  $\Xi$ . We can always decompose the perturbation into its components in the local eigenvector basis, i.e. in two parts. One part, describing the rate of change in the slow subspace and one describing the rate of change in the fast subspace. Now let us assume that the time-scale of the perturbation is of the order of the time scales of the slow movement within the manifold, i.e. much smaller than those of the

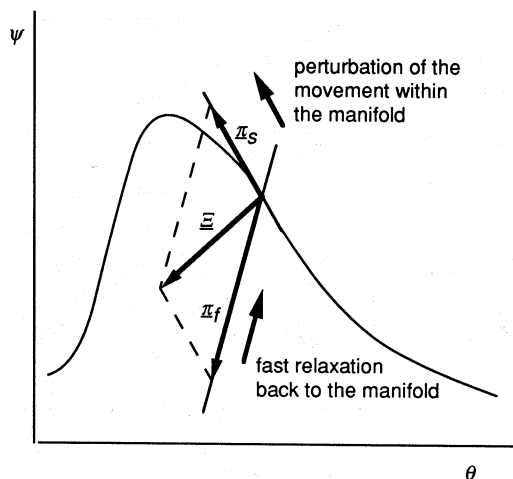


FIG. 4. Schematical illustration of a perturbation process.

fast relaxing time scales. This is what will happen: The components of the perturbation in the direction of the fast subspace will have a minor effect on the chemical reaction system, because chemistry (fast equilibration processes) relaxes the perturbation back to the manifold. The components of the perturbation in the slow subspace instead, will directly couple with the time scales of the chemical reaction and thus move the state within the manifold. That means if we project the perturbation locally onto the slow subspace, we can account for the interaction of the physical processes with the slow time scales, whereas we neglect all processes which perturb the chemistry, but are "equilibrated" by the chemistry within a very short time (of the order of the fast time scales).

Using those ideas, we can formulate a projection operator  $P$ , which depends on the local characteristics of the manifold and which projects a physical perturbation  $\Xi(\psi)$  onto a perturbation  $I(\theta)$  within the manifold (see appendix). This means that all we have to know in order to solve the coupled problem are the rates of change of the parameters  $S(\theta)$ , the state space  $\psi(\theta)$  and the local projection matrices  $P(\theta)$  as functions of the parameters  $\theta$ . The method described above will work and yield good approximations as long as the time scales of the perturbations are slow compared with the fast relaxing time scales which had been decoupled by the construction of the intrinsic low-dimensional manifold. Note that there has not been made any restriction to the kind of perturbation. It could be, e.g. be caused by diffusion processes, mixing processes etc.

In order to show the validity and the limits of applicability of this approach, we have performed

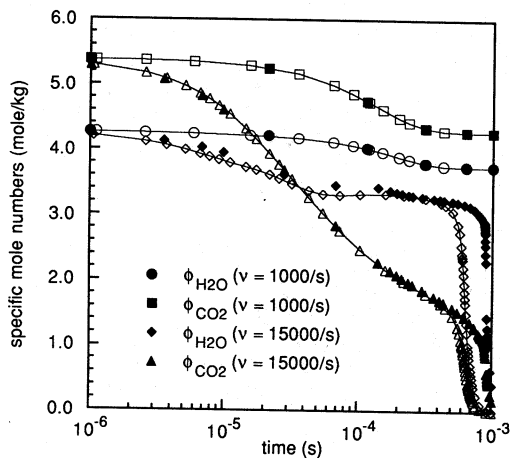


FIG. 5. Plot of the specific mole numbers of  $\text{CO}_2$  and  $\text{H}_2\text{O}$  versus time for a  $\text{CO}/\text{H}_2/\text{air}$  system in a flow reactor for mixing rates of  $\nu = 1,000$  1/s and  $\nu = 15,000$  1/s (see text for details on the reaction system and the initial values); empty symbols denote detailed chemical kinetics, full symbols denote the reduced kinetics results.

sample calculations for a test case, namely the model of a perfectly stirred flow reactor. In this case the system is constantly perturbed by mixing with an unburnt gas mixture. The governing equation system is given by:

$$\frac{\partial \underline{\psi}}{\partial t} = \underline{F}(\underline{\psi}) + \nu(\underline{\psi}^m - \underline{\psi}) \quad (5)$$

where  $\underline{\psi}^m$  denotes the state of the mixing gas entering the reactor, and  $\nu$  the rate of mixing. The mixture considered has been described in chapter 3. In the sample calculations, the initial composition of the mixture had been taken as the equilibrium value, for the mixing gas an unburnt mixture of  $\text{CO}$ ,  $\text{H}_2$  and air with the same enthalpy, pressure and element composition as that in the reaction vessel has been used. Of course other conditions can be handled, too, and various sample calculations all show the same behavior as the system discussed in this paper. Both, reduced and detailed chemical rate equations were integrated using an implicit extrapolation code<sup>15</sup> with internal order and stepsize control and error estimation. Plotted in Figs. 5 and 6 are the specific mole numbers of  $\text{CO}_2$  and  $\text{H}_2\text{O}$  versus time. The mixing rate has been varied over a wide range. Shown are only values of 1,000, 10,000 and 15,000 1/s. For the case of a mixing rate of 1,000 1/s detailed and reduced chemical kinetics are almost identical. Increasing the rate of mixing narrows the gap between the time

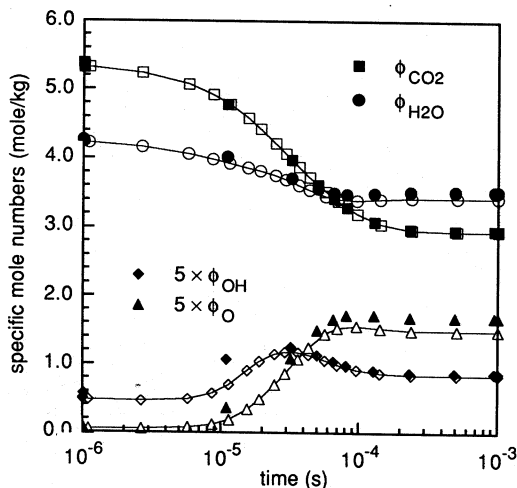


FIG. 6. Plot of the specific mole numbers of  $\text{CO}_2$ ,  $\text{H}_2\text{O}$ ,  $\text{O}$  and  $\text{OH}$  versus time for a  $\text{CO}/\text{H}_2/\text{air}$  system in a flow reactor, mixing rate  $\nu = 10,000$  1/s; empty symbols denote detailed chemical kinetics, full symbols denote the reduced kinetics results.

scale of mixing and the decoupled fast time scales. Thus the error of the simplified scheme increases slightly. Fig. 6 shows (for  $\nu = 10,000$  1/s) plots of the radicals  $\text{O}$  and  $\text{OH}$ , and it can be seen, that our method not only describes the development of major species very well, but also minor species, which is an important issue e.g. in modelling pollutant formation.

The behaviour of the reaction system for  $\nu = 15,000$  1/s deserves a special discussion. In this case mixing with unburnt gas leads to extinction. This process (which is an important issue in turbulent flame computations) is captured by the reduced mechanism, too. However, the increase of the mixing rate to 15,000 1/s leads to compositions, where the local time scales which had been decoupled become very close to the time scale of mixing, and thus the reduced scheme is inaccurate during the transition process (right side of the diagram). But the onset of extinction and the final state (unburnt mixture in the reaction vessel) are simulated correctly even in this case. The conclusions which can be drawn from this behaviour are: The scheme works very well if the time scale of the physical process (e.g. diffusion or mixing) is reasonably slower than the fast decoupled time scales. If the gap between the fast time scales and the time scale of the coupling physical process becomes too narrow, a higher dimensional table has to be used. Increasing the dimension of the table simply changes the slowest of the fast time scales into a slow (and thus controlling) time scale. Fig. 7 shows a plot of the negative eigenvalues versus time for  $\nu = 15,000$  1/s

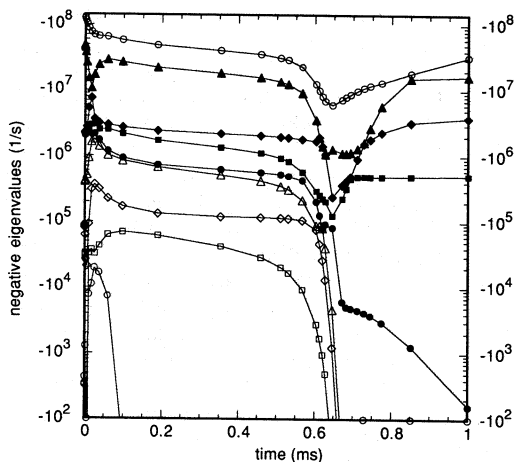


FIG. 7. Eigenvalue spectrum versus time for mixing rate  $\nu = 15,000$  1/s.

and allows to determine the dimension of the manifold needed to capture different time scales. Thus, even if we are e.g. interested to capture processes occurring at time scales of  $10^5$  1/s (corresponding to a time of  $100 \mu\text{s}$ ), we can decouple 6 fast time scales (namely those corresponding to eigenvalues  $< -5 \cdot 10^6$  1/s), at least in the time interval before the extinction process.

One further feature is the influence of the reduction procedure on the numerical integration of the rate equations. One effect is the reduction of the dimension of the system. Whereas for the example above 15 coupled ordinary differential equations have to be solved in the detailed kinetics scheme, the reduced scheme only needs the treatment of two equations. Furthermore, time consuming computation of the chemical rate equations is replaced by a simple table lookup. In the example above, the cpu time for the reduced rate equations is only about 6% of the cpu time needed for the detailed chemistry calculation. Not only is the dimension of the system reduced considerably, but also along with decoupling the fast time scales, much of the stiffness of the governing equation system is eliminated. This allows (at least in some cases) the use of explicit methods in the CFD computations. Furthermore, very often in CFD codes not the chemical rates of production are needed, but the changes of composition in certain time intervals. In this case, these increments can be stored in the table, too, avoiding any integration of the rate equations in the CFD code.

### Appendix

In order to obtain a mathematical formulation for the coupling of the reduced chemistry scheme with

physical processes, let us start with the general formulation of a chemical reaction system perturbed by some physical processes:

$$\frac{\partial \psi}{\partial t} = \underline{F}(\psi) + \underline{\Xi}(\psi) \quad (\text{A.1})$$

where  $\underline{F}(\psi)$  denotes the chemical rates of change and  $\underline{\Xi}(\psi)$  the physical perturbation. The state  $\psi$  itself is a function of the  $N$  parameters  $\theta$  which parametrize the manifold. If  $\underline{\Xi}(\psi)$  is the perturbation, its components in the local eigenvector basis  $V$  (see 6,7) are given by:

$$\underline{\pi} = (\pi_1, \pi_2, \dots, \pi_n) = V^{-1} \underline{\Xi}(\psi). \quad (\text{A.2})$$

Having sorted the eigenvectors according to decreasing real part (see above),  $\underline{\pi}$  is given by  $\underline{\pi} = (\underline{\pi}_s, \underline{\pi}_f)^T$  where  $\underline{\pi}_s$  and  $\underline{\pi}_f$  denote the vectors of the components in the slow and the fast subspace, respectively.

Noting that the perturbations in the fast subspace relax to zero, the approximation of the perturbation is given by:

$$\bar{\underline{\pi}} = (\underline{\pi}_s, 0)^T = \begin{pmatrix} I & 0 \\ 0 & 0 \end{pmatrix} V^{-1} \underline{\Xi}(\psi), \quad (\text{A.3})$$

where  $I$  denotes an  $N \cdot N$  dimensional identity matrix and the zeros denote that all other elements of the matrix are zero. Transformation back into the natural basis yields for the "effective perturbation":

$$\bar{\underline{\Xi}}(\psi) = V \begin{pmatrix} I & 0 \\ 0 & 0 \end{pmatrix} V^{-1} \underline{\Xi}(\psi). \quad (\text{A.4})$$

Making use of the parametrization of the manifold, which (for simplicity) shall be given by  $\theta = C\psi$ , where  $C$  denotes an  $N \cdot n$ -dimensional parametrization matrix, we obtain for the equation system (1):

$$\frac{\partial \theta}{\partial t} = C\underline{F}(\psi) + C\underline{\Xi}(\psi) = \underline{S}(\theta) + P\underline{\Xi}(\psi(\theta)), \quad (\text{A.5})$$

where  $P$  denotes the projection matrix:

$$P = CV \begin{pmatrix} I & 0 \\ 0 & 0 \end{pmatrix} V^{-1} \quad (\text{A.6})$$

### Acknowledgements

Financial support by General Electric and the BMFT (in the frame of the *TECLAM*-Project) is gratefully acknowledged.

## REFERENCES

1. DIXON-LEWIS, G., DAVID, T., GASKELL P. H., FUKUTANI, S., JINNO, H., MILLER, J. A., KEE, R. J., SMOOKE, M. D., PETERS, N., EFFELSBURG, E., WARNATZ, J. AND BEHRENDT, F.: Twentieth Symposium (International) on Combustion; p. 1893, 1985.
2. WARNATZ, J.: Eighteenth Symposium (International) on Combustion, p. 369. The Combustion Institute, 1981.
3. SMOOKE, M. D., MITCHELL, R. E. AND KEYES, D. E.: *Combust. Sci. Tech.* 67, 85 (1989).
4. WARNATZ, J. AND MAAS, U.: Calculation of the Detailed Structure of Premixed and Non-Premixed Flame Fronts and Some Applications, IMACS Transactions on Scientific Computing '88, in: *Numerical and Applied Mathematics*, (W. F. Ames (Ed.)) J. C. Baltzer AG, Scientific Publishing Co., p. 151 (1989).
5. *Reduced Kinetic Mechanisms and Asymptotic Approximations for Methane-Air Flames* (M. D. Smooke, Ed.), *Lecture Notes in Physics 384*, Springer (1991).
6. MAAS, U. AND POPE, S. B.: *Simplifying Chemical Kinetics: Intrinsic Low-Dimensional Manifolds in Composition Space*, *Combust. Flame* 88, p. 239 (1992).
7. MAAS, U. AND POPE, S. B.: *Simplifying Chemical Kinetics: Intrinsic Low-Dimensional Manifolds in Composition Space*, IWR, University of Heidelberg, Tech. report no. 91-22, Heidelberg, FRG (1991).
8. LAM, S. H. AND GOUSSIS, D. A.: *Twenty-Second Symposium (International) on Combustion*, p. 931, The Combustion Institute, 1989.
9. LAM, S. H. AND GOUSSIS, D. A.: *Conventional Asymptotics and Computational Singular Perturbation for Simplified Kinetics Modelling*, Technical Report #1864(a)-MAE, Princeton University, USA (1990).
10. CHEN, J-Y. AND DIBBLE, R. W.: in *Reduced Kinetic Mechanisms and Asymptotic Approximations for Methane-Air Flames* (M. D. Smooke, Ed.), *Lecture Notes in Physics 384*, Springer (1991).
11. POPE, S. B.: *Eighteenth Symposium (International) Combustion*, p. 1001, The Combustion Institute, 1981.
12. PRESS, W. H., FLANNERY, B. P., TEUKOLSKY, S. A. AND VETTERLING, W. T.: *Numerical Recipes*, Cambridge University Press, ISBN 0521383307 (1989).
13. MAAS, U. AND WARNATZ, J.: *Twenty-Second Symposium (International) on Combustion*, p. 1695, The Combustion Institute 1989.
14. MAAS, U. AND POPE, S. B.: publication in preparation
15. DEUFLHARD, P. AND NOWAK, U.: *Extrapolation Integrators for Quasilinear Implicit ODEs*. SFB 123 Tech. Rep. 332, University of Heidelberg, Heidelberg, FRG (1985).

## COMMENTS

*Michael Tanoff, Chalmers University of Technology, Sweden.* Often, the terms "reduced chemistry" or "reduced kinetic mechanism" call to mind "global" or "overall" chemical reactions, such as the water-gas shift reaction,  $\text{CO} + \text{H}_2\text{O} \rightarrow \text{CO}_2 + \text{H}_2$ . Your intrinsic low-dimensional manifolds do not seem to explicitly reveal such physically descriptive chemistry. It is possible to extract conventional overall chemical reactions from your resulting manifold space, or are such chemical steps imbedded too deeply in the mathematical formulation of your method?

*Author's Reply.* The aim of our method is to provide a numerical algorithm for reducing chemical kinetics. However, the method can also reveal information about the chemistry. Having identified the low-dimensional manifold, we obtain all states of the system which correspond to equilibrium with respect to the fastest relaxing time scales, i.e. the manifold reveals all states where some kind of par-

tial equilibrium or steady state exists. If we analyze the eigenvectors of the Jacobian for given states which lie on the manifold, we can obtain information about the underlying chemical processes. It turns out that the quite abstract eigenvectors are simply some linear combinations of chemically meaningful vectors (e.g. reaction vectors denoting the rate of change according to certain elementary reactions, species vectors denoting the rate of change of certain species (see Ref. 1)). If, for example, an eigenvector with a large negative eigenvalue corresponds to a reaction vector of an elementary reaction, this implies that this reaction is in partial equilibrium.

Usually partial equilibrium and steady state conditions change with changing conditions, but because the ILDM method maps the whole-thermochemical state space, it captures those changes and thus provides information concerning the optimal assumptions in the different regimes.



## REFERENCE

1. MASS, U. AND POPE, S. B.: Simplifying Chemical Kinetics: Intrinsic Low-Dimensional Manifolds in Composition Space, *Combust. Flame* 88, 239 1992.

A. K. Oppenheim, *University of California, Berkeley, USA*. The paper provides a beautiful recognition of the fact that thermochemistry of combustion is a nonlinear process whose essential properties are described in terms of an ODE system. The solution is an integral curve (trajectory) in a phase space. Characteristic features of these curves and, especially, of their manifolds and singularities one of obvious interest, as, indeed, the paper demonstrates. Singularities are particularly prominent with respect to the concentration of a significant active radical as a reference coordinate, as reflected by the studies of Brian Grey, Peter Grey, John Griffiths and their associates at Leeds. Have you taken these aspects into account in the course of your studies?

*Author's Reply.* The nonlinear character of chemical kinetics, which is reflected by the mathematical properties of the governing ordinary differential equation system, leads to interesting phenomena both from a mathematical as well as from a chemical point of view. The qualitative theory of ordinary differential equation systems, dating back to the work of Poincare, Liapunov, Picard and others, can provide useful information about stability, oscillatory behaviour, etc. Analysis of the stationary states of a chemical reaction system were, e.g., successfully used to explain the oscillatory and explosive behaviour in the oxidation of carbon monoxide (see e.g. 1-3).

The method that we presented exploits the fact that besides the information obtained by mathematical methods for stationary points, analysis of the ODE system can, in addition, provide information about how (i.e. along which path) the chemistry approaches equilibrium. Simply stated our method connects the stationary points by manifolds which act as attractors for trajectories. The manifolds themselves are sets of points with partial equilibrium ("stationarity") with respect to the fastest relaxing time scales and thus can represent the interesting dynamic behaviour of the chemical reaction system.

## REFERENCES

1. GRAY, B. F.: *Trans. Faraday Soc* 66, 1118 1970.  
2. YANG, C. H.: *Combust. Flame* 23, 97 1974.

3. BOND, J. R., GRAY, P., GRIFFITHS, J. F. AND SCOTT, S. K.: *Proc. R. Soc. Lond. A* 381, 293 1982.

S. H. Lam, *Princeton University, USA*. The method of Computational Singular Perturbation (CSP<sup>1</sup>) and ILDM exploit the same basic idea: suppress the fast modes when they are exhausted by finding and using the basis vectors of the fast manifold. The implementations are different, and I believe the ILDM implementation has certain fundamental shortcomings.

Let's formally decompose  $\mathbf{F}(\psi)$  into its fast and slow components:

$$\mathbf{F}(\psi) = \mathbf{F}(\psi)^{\text{fast}} + \mathbf{F}(\psi)^{\text{slow}}. \quad (1)$$

While theoretically  $\mathbf{F}(\psi)^{\text{slow}}$  can be evaluated by either

$$\mathbf{F}(\psi)^{\text{slow}} = \mathbf{F}(\psi(\theta)) \quad (2)$$

or

$$\mathbf{F}(\psi)^{\text{slow}} = \mathbf{V} \begin{vmatrix} \mathbf{I} & 0 \\ 0 & 0 \end{vmatrix} (\mathbf{V})^{-1} \cdot \mathbf{F}(\psi), \quad (3)$$

the numerical accuracy requirement of  $\psi = \psi(\theta)$  for (2) is *unreasonably more severe* than for (3). Let  $\epsilon$  denote the ratio of the fast over the slow time scales. Mathematically, the algorithm being advocated by Maas and Pope, (2), requires  $\psi = \psi_o(\theta) + \epsilon\psi_1(\theta) + O(\epsilon^2)$ , and its small  $O(\epsilon)$  component (i.e.  $\psi_1(\theta)$ ) is crucial and must be accurately evaluated. This (theoretically correct) algorithm is simply not numerically viable for problems with very large time-scale separations (i.e.  $\epsilon \ll 1$ ).

The CSP method advocated by myself and Goussis uses a variant of (3) which has the normal accuracy requirement (i.e.  $\psi = \psi_o(\theta) + O(\epsilon)$ ) but does not require the calculation of the slow eigen-vectors.

## REFERENCE

1. GOUSSIS, D. A. AND LAM, S. H.: A Study of Homogeneous Methanol Oxidation Kinetics Using CSP, Twenty-Fourth Symposium on Combustion, The Combustion Institute, 1992.

*Author's Reply.* Indeed ILDM and CSP exploit some of the same basic ideas, but not only the implementation, but also the results obtained by the methods are different. Both methods can be used to obtain information about the chemical reaction system (species in steady state, partial equilibrium reactions, etc.). But this is not the main motivation

for using the ILDM method. CSP makes use of the fact that, during the course of a chemical reaction, certain fast modes can be suppressed if they are exhausted. This reduces the stiffness of the problem and allows the use of explicit methods for the integration of the chemical rate equations. However, the governing equation system that has to be solved, still has a dimension corresponding to the number of chemical species. In practical applications (e.g. three-dimensional turbulent flames), one is not only interested in reducing the stiffness, but the complexity of the problem requires a reduction of the number of variables which govern the chemical reaction system (this number corresponds to the number of partial differential equations that have to be solved in order to simulate the reacting flow). Our ILDM method thus, in contrast to CSP, reduces (based on an eigenvector analysis) the state space globally such that the chemical reaction can be expressed in terms of a small number of reaction

progress variables. The results can be used in subsequent reacting flow calculations.

In the comment the accuracy requirement is discussed. It is stated that (2) has a higher accuracy requirement than (3). Specifically Prof. Lam himself states that the accuracy requirement for  $\psi$  in (2) is

$$\psi = \psi_0(\theta) + \epsilon\psi_1(\theta) + O(\epsilon^2) \quad (1)$$

Thus for problems with very large time scale separations (i.e.,  $\epsilon \ll 1$ ) the method will work very well. Numerical experiments for the examples presented in the paper show that the values obtained numerically for  $\mathbf{F}(\psi)^{\text{slow}}$  using (2) or (3) show almost no difference. Furthermore (if it really were necessary), (3) could be readily used for the evaluation of  $\mathbf{F}(\psi)^{\text{slow}}$ , because all information is obtained as output of the ILDM method. From this discussion we conclude that there is no basis for the belief that the ILDM implementation has certain fundamental shortcomings.